

## Persistent Holes in a Fluid

Florian S. Merkt, Robert D. Deegan, Daniel I. Goldman, Erin C. Rericha, and Harry L. Swinney

*Center for Nonlinear Dynamics, The University of Texas at Austin, Austin, Texas 78712, USA*

(Received 10 November 2003; published 5 May 2004)

We observe stable holes in a vertically oscillated 0.5 cm deep aqueous suspension of cornstarch. Holes appear only if a finite perturbation is applied to the layer for accelerations  $a$  above  $10g$ . Holes are circular and approximately 0.5 cm wide, and can persist for more than  $10^6$  cycles. Above  $a \approx 17g$  the rim of the hole becomes unstable, producing fingerlike protrusions or hole division. At higher acceleration, the hole delocalizes, growing to cover the entire surface with erratic undulations. We find similar behavior in an aqueous suspension of glass microspheres.

DOI: 10.1103/PhysRevLett.92.184501

PACS numbers: 47.50.+d, 47.20.-k, 47.54.+r, 47.55.Kf

The free surface of a fluid at rest in a container is flat. Departures from flatness induce a restoring flow whether the fluid is Newtonian, viscoelastic, or liquid crystalline: poke the surface, and the resulting indentation will be filled by the ensuing flow. In contrast, we have discovered that a vibrated aqueous suspension of cornstarch or glass microspheres can permanently support holes and vertical fingerlike protrusions.

The catalog of interface morphologies in accelerated fluids is broad and well documented. Sinusoidal acceleration produces Faraday waves [1], solitons [2,3], and jets [4]. Impulsive acceleration produces the Richtmyer-Meshkov instability [5,6], and continuous acceleration the Rayleigh-Taylor [7] instability, characterized by spires and bubbles [8]. In contrast, holes and fingers do not exhibit the oscillation about a flat state of Faraday waves and solitons, the finite lifetime of jets, or the unbounded growth of the Richtmyer-Meshkov or Rayleigh-Taylor instabilities.

Figure 1 shows holes in vibrated aqueous suspensions of cornstarch 1(a) and 1(b) and glass microspheres 1(d) and 1(e). Depending on the container acceleration and frequency, the initial fluid surface is either flat or corrugated by Faraday waves. Above a critical acceleration, a finite localized perturbation of the fluid surface grows into a stable cylindrical void that extends from the top to nearly the bottom of the fluid layer. The most noteworthy feature of holes is their permanence: they do not close despite the hydrostatic pressure of the surrounding fluid, persisting as long as our observations ( $>10^6$  cycles). At yet higher accelerations, the holes lose stability to a temporally and spatially erratic state [see Figs. 1(c) and 1(f)].

*Experiment.*—A layer of cornstarch or glass microspheres in liquid was vertically oscillated sinusoidally with a frequency  $f$  from 50 to 180 Hz and a peak acceleration  $a$  up to  $27g$  (controlled to  $\pm 0.01g$ ). The container had an aluminum base plate, acrylic sidewall (inner diameter 9.4 cm), and acrylic top. The container was sealed to reduce evaporation and was attached to the shaker through an insulating rod to avoid heat transfer from the shaker to the container. The layer depth was 0.5 cm

for the cornstarch mixture and 0.2 cm for the glass microspheres.

The patterns were recorded with 30 and 2000 frames/second cameras. Lighting in Fig. 1 was provided by a ring

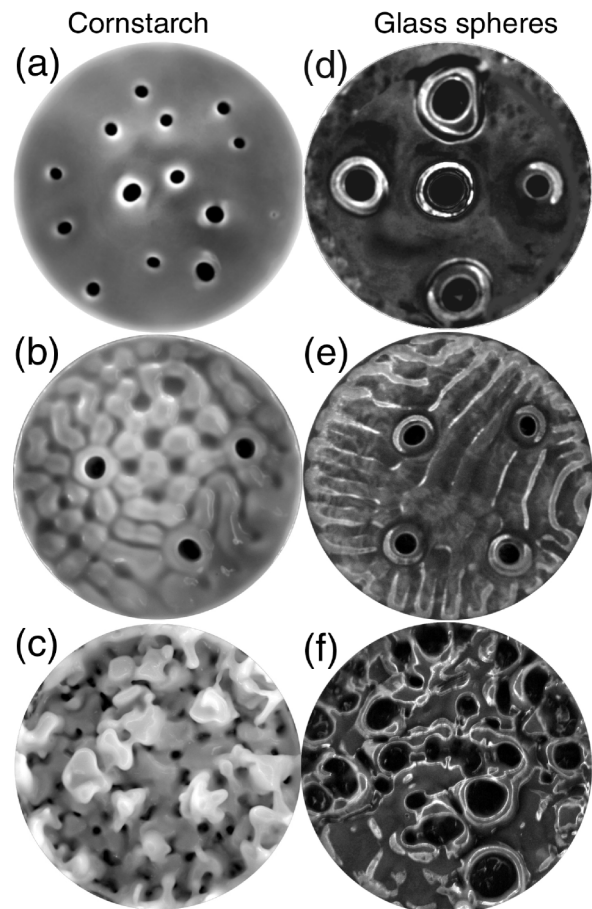


FIG. 1. Top view of a vibrated layer of an aqueous suspension of (a)–(c) cornstarch and of (d)–(f) glass microspheres (image diameter, 9.4 cm). White corresponds to the highest points, and black to depressions that reach near the container bottom. Holes without Faraday waves: (a)  $a = 12g$ ,  $f = 150$  Hz; (d)  $30g$ ,  $100$  Hz. Holes with Faraday waves: (b)  $12g$ ,  $60$  Hz; (e)  $27.3g$ ,  $92$  Hz. Delocalized state: (c)  $30g$ ,  $120$  Hz; (f)  $30g$ ,  $60$  Hz.

of light-emitting diodes strobed at  $f$  or  $f/2$ . The illumination was such that peaks on the surface appear bright and valleys dark. The layer was lit from above for the measurements of the size of the holes. The hole shape was determined by illuminating a narrow section of the hole with a sheet of laser light projected perpendicular to the layer surface, and photographing from an angle the deviations from straightness of the laser line.

We used cornstarch consisting of 27% amylose and 73% amylopectin from Sigma Aldrich. The powder was dried at 50 °C for a week and stored in a desiccator. A mixture was prepared daily by combining 23.22 g of cornstarch and 36.78 g of a density-matched aqueous solution of CsCl with a density of 1.68 g/cm<sup>3</sup>. The quantitative results we present are for cornstarch, but we also used glass microspheres in an aqueous solution for the qualitative comparison in Fig. 1. The glass mixture was prepared with 29.37 g of glass balls (1–20  $\mu$ m) from Jaygo (Union, NJ), and 18.36 g of an aqueous solution of sodium polytungstate with a density of 2.55 g/cm<sup>3</sup>.

*Hole dynamics and size selection.*—The interface of a vibrated fluid is flat at low accelerations and rippled by Faraday waves above a critical acceleration [1]. Holes persist in the cornstarch mixture only if an indentation deeper than about 50% the layer depth and 0.4–2.0 cm wide is applied to the surface. Holes were generated with a puff of air through a nozzle pointed at the surface. The subsequent evolution of a hole depends on the parameters  $a$  and  $f$ . For all parameter values explored, the hole may

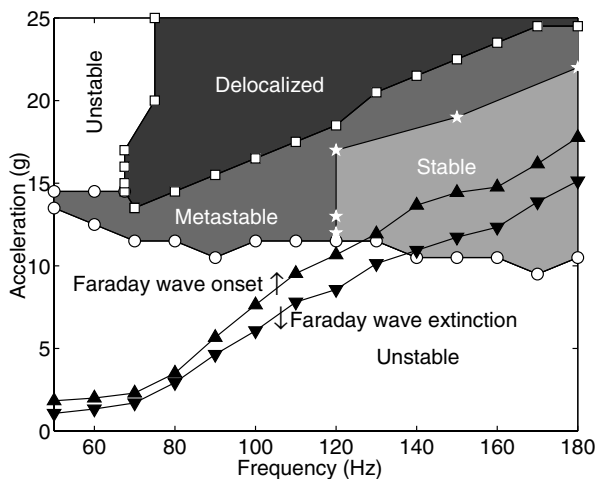


FIG. 2. Phase diagram for a vibrated aqueous cornstarch suspension as a function of acceleration and frequency. In either the metastable or stable region, a surface perturbation forms a persistent hole. In the metastable regime these holes always collapse within  $10^5$  container oscillations; in the stable regime some holes last for more than  $10^5$  oscillations. In the areas marked unstable, holes collapse in less than  $10^4$  cycles. In the delocalized regime the surface is highly irregular, as shown in Fig. 1(c). Faraday waves appear with increasing acceleration at ▲, and disappear with decreasing acceleration at ▼.

close within seconds. In the region of the phase diagram (Fig. 2) marked “unstable” all holes decay in this way. In regions marked “stable” and “metastable,” holes adjust to a size that has a fairly well-defined average value (Fig. 3), but over extended periods of time the size slowly wanders within a 30% band. At  $f = 120$  Hz the characteristic hole diameter is 0.4 cm, and at  $f = 180$  Hz, 0.6 cm. Holes have a broad distribution of lifetimes, even for fixed  $f$  and  $a$ ; in the metastable phase the maximum lifetime is less than  $10^5$  cycles, and in the stable phase it is greater than  $10^5$  cycles. The value of  $10^5$  cycles was selected as the cutoff for stable holes because holes that live that long will almost always live for more than  $10^6$  cycles.

Short-lived holes collapse within a few seconds by a uniform contraction. Holes lasting longer than about  $10^4$  oscillations develop a hump on their rims, which then falls onto the hole, either covering it or rendering it so small that it collapses rapidly by uniform contraction. On occasion this latter mechanism causes the hole to divide rather than collapse.

Holes typically have a nearly circular horizontal cross section [see Fig. 1(a)]. Vertical cross sections through hole centers are shown in Fig. 4(a). At the base of the hole, there is usually a ribbon of material about 0.1 mm high and 2 mm wide that bisects the shaft, as seen in the solid line in Fig. 4(a). This feature is not visible in all of the radial profiles because it is not azimuthally symmetric and may be missed in a single profile of the hole. At accelerations immediately above the stability line the material surrounding a hole remains level with the rest of the layer, while at higher acceleration, the hole’s rim rises about 0.5 mm above the surrounding fluid.

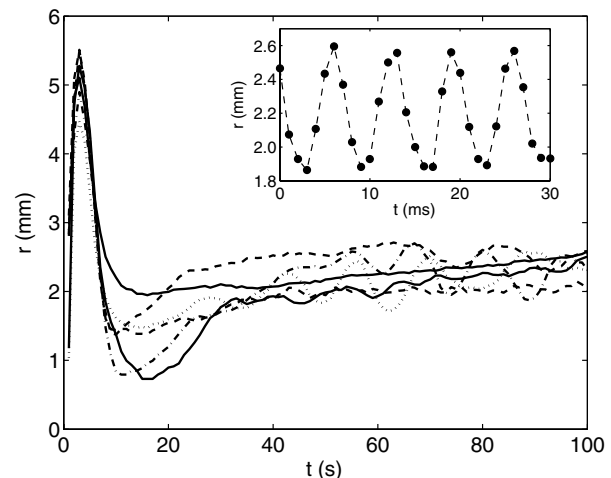


FIG. 3. Time evolution of the radii of six holes formed with a 2 s long puff of air. Holes grow during the forcing and then rapidly shrink after the air is cut off. Inset: hole diameter oscillates synchronously with the forcing; note time scale ( $a = 15g$ ,  $f = 150$  Hz).

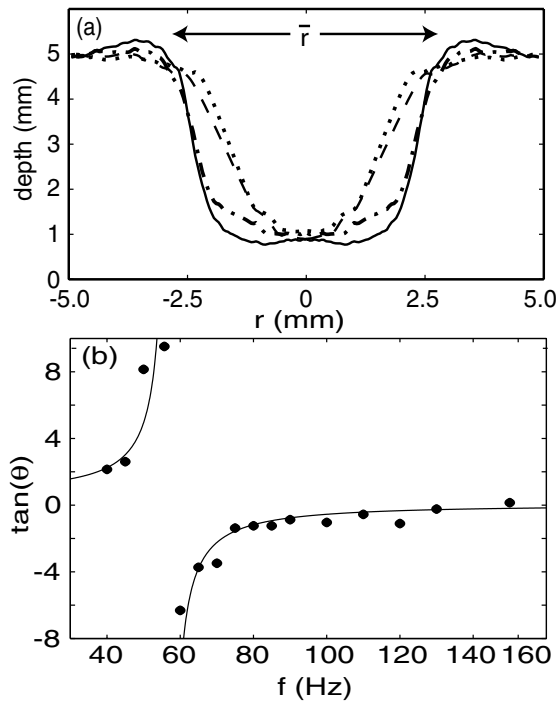


FIG. 4. (a) Vertical cross sections of holes at  $a = 14.5g$  (dashed and dotted lines) and  $a = 17g$  (solid and dot-dashed lines) for  $f = 150$  Hz. The two profiles for each acceleration show the extremes in a hole's shape, separated by one-half cycle. (b) The tangent of the phase lag versus frequency at  $a = 15g$ . The solid line is a fit to  $\alpha/[1 - (f/f_0)^2]$ , where  $\alpha$  and  $f_0$  are fitting parameters.

In addition to a slow variation over hundreds of oscillations, the radius  $r(t)$  of a hole oscillates synchronously with the driving frequency (inset of Fig. 3):  $r(t) = \bar{r} + \delta r \sin(2\pi ft + \theta)$ , where  $\bar{r}$  is the mean radius,  $\delta r$  is the amplitude of the oscillation, and  $\theta$  is the phase relative to the container motion  $z(t) = z_0 \sin(2\pi ft)$ , where  $z_0 = -a/(2\pi f)^2$  and  $z > 0$  when the container is above its rest point.  $\delta r$  is typically  $0.15\bar{r}$ . The phase lag is shown as a function of frequency in Fig. 4(b).

Holes do not interact when their centers are separated by more than about two diameters. Therefore, as shown in Fig. 1(a), holes do not form regular patterns. Further, they can be located anywhere in the container. Holes occasionally come sufficiently close to interact, and then they merge or annihilate.

*Faraday waves.*—Though Faraday waves are excited in cornstarch suspensions, the formation of holes is unrelated to these waves, as can be seen from the existence of holes when no Faraday waves are present [Figs. 1(a) and 1(d)]. Further, the phase boundaries for holes and Faraday waves are distinct. The Faraday transition is hysteretic, and, moreover, the flat and surface wave state can coexist. As  $a$  is increased at a fixed  $f$ , small patches of surface waves appear at the boundary “Faraday wave onset” in Fig. 2. As  $a$  is raised further, the patches grow and

ultimately engulf the entire surface at  $a$  values typically 50% higher than onset. With decreasing  $a$ , the surface waves break up into patches that finally disappear at the boundary “Faraday wave extinction” in Fig. 2.

*Delocalization.*—In the “delocalized” region in Fig. 2, a perturbation generates a hole that immediately grows a protrusion from its rim, as Fig. 5 illustrates. The protrusions can rise as high as 2 cm and remain upright for thousands of oscillations before falling and nucleating a new hole. The process continues until the entire surface writhes with fingers and holes, yielding the spatially and temporally erratic state shown in Figs. 1(c) and 1(f). The transition from the metastable hole region to the delocalized state is not hysteretic. If  $a$  is decreased through the value for delocalization onset, the erratic motion ceases and the irregular pattern imprinted by the delocalized state evolves according to hole dynamics.

*Shear thickening.*—We attribute the stability of holes to shear thickening, i.e., an increase of viscosity with shear rate. We measured the viscosity of the cornstarch suspension (Fig. 6) and found a behavior typical of shear thickening fluids [9]; i.e., an initial decrease of the viscosity for increasing shear rate is followed by a rapid increase at a critical shear rate, which in this case is  $\dot{\gamma}_c = 8 \text{ s}^{-1}$ . Our conclusion is predicated on four observations: the critical shear rate is similar in magnitude to the shear rate at the throat of a hole; the phase lag of the hole's radius relative to the driving force indicates the material response is primarily viscous; holes are unstable in a nonshear thickening fluid; and holes are stable in shear thickening fluids other than cornstarch suspensions.

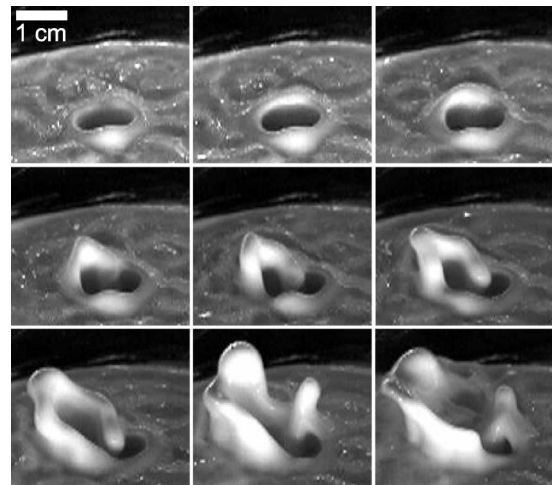


FIG. 5. Side view of the first steps toward the delocalized state in cornstarch. These photographs were taken every 0.9 s; time increases from left to right and top to bottom. An initial hump on the rim begins growing upward, reaches a maximum height, and then topples outward, enlarging the area of fluid motion. This process repeats until the entire surface of the liquid is active in the creation and destruction of vertical structures and voids [see Fig. 1(c)] ( $a = 25g$ ,  $f = 80$  Hz).

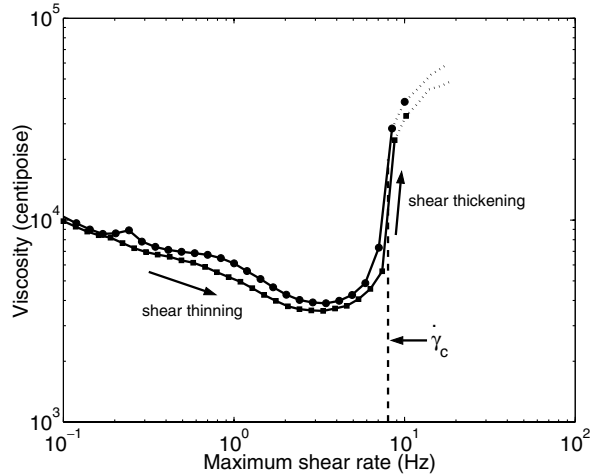


FIG. 6. Apparent viscosity as a function of the maximum shear rate  $\dot{\gamma}$  for two cornstarch suspensions prepared in the same manner as in Fig. 1. Measurements were made with a plate-plate rheometer (Paar Physica TEK 150) with radius  $R = 2.5$  cm and gap 0.1 cm. The apparent viscosity was calculated as for a Newtonian fluid:  $\eta = 2\tau/(\pi\dot{\gamma}R^3)$  where  $\tau$  is the torque. Since the shear rate increases with the radius, our measurement of the viscosity is a convolution of the geometry and the response of the fluid. The dashed extension of the curve represents measured values that are not reliable due to an instability in the flow (temperature,  $27.6 \pm 0.2$  °C).

We can estimate the shear rate for an oscillating hole (inset of Fig. 3). The root-mean-square shear rate at throat of the hole is approximately the interface speed,  $(2\pi/\sqrt{2})\delta r f$ , divided by a length scale of order the depth of the layer  $h$ . Using  $\delta r/\bar{r} \approx 0.15$ ,  $f = 100$  Hz, and  $\bar{r}/h \approx 0.4$ , we obtain  $\dot{\gamma} \approx 27$  s $^{-1}$ . The similarity of this value to the critical shear rate strongly suggests that shear thickening is an essential ingredient for holes.

The frequency dependence of the phase lag  $\theta$  indicates a combined viscous and elastic response of the fluid. Modeling the hole motion as a spring in parallel with a dashpot (i.e., a Voigt element; see [10], for example) yields  $\tan\theta = \alpha/[1 - (f/f_0)^2]$ , where  $\alpha$  is a constant proportional to the dissipation and  $f_0$  is the resonant frequency. As shown in Fig. 4(b), the data are well modeled by this equation; the resonance frequency is around 58 Hz. Since the Voigt element is primarily viscous at high frequency, the phase data indicate that at frequencies above 60 Hz the material response becomes dominantly viscous; it is noteworthy that stable holes form only in this high frequency region.

We also tried to form persistent holes in a Newtonian fluid (silicone oil with a viscosity of 3.4 P) and viscoelas-

tic fluids (polybutadienes with viscosities of 8.3, 28, and 72 P). In all cases, however, an initial hole was backfilled within a few hundred container oscillations.

Barnes [9] states that any sufficiently concentrated suspension of solids in a fluid will shear thicken. If shear thickening is crucial for hole formation, then any sufficiently dense suspension of solids ought to support persistent holes. Indeed, we conducted experiments on a dense suspension of glass microspheres and found the hole and delocalized states, as shown in Figs. 1(d) and 1(e).

*Conclusions.*—We have shown that a vertically vibrated aqueous suspension of cornstarch displays a number of unexpected patterns—holes, fingers, and a delocalized state—that can be attained only by the application of a finite perturbation. Holes vibrate synchronously with the container and are unrelated to the well-known Faraday waves. At higher acceleration the hole becomes unstable to the creation of fingerlike structures, which at even higher accelerations are responsible for the transition to an irregular delocalized state. Outstanding questions include the following: How do holes stay open? What sets their size? How can the fingerlike protrusions grow and remain upright? What drives the transition to the delocalized state?

We thank M. Schröter, W. D. McCormick, P. Heil, A. Lee, W. Zhang for valuable suggestions, and P. Green and A. Jamieson for assistance with the viscosity measurements. We acknowledge support by the Engineering Research Program of the Office of Basic Energy Sciences of the U.S. Department of Energy under Grant No. DE-FG03-93ER14312. F. S. M. acknowledges support by the Friedrich Ebert Stiftung.

- 
- [1] M. Faraday, *Philos. Trans. R. Soc. London* **121**, 299 (1831).
  - [2] O. Lioubashevski, H. Arbell, and J. Fineberg, *Phys. Rev. Lett.* **76**, 3959 (1996).
  - [3] O. Lioubashevski, Y. Hamiel, A. Agnon, Z. Reches, and J. Fineberg, *Phys. Rev. Lett.* **83**, 3190 (1999).
  - [4] M. S. Longuet-Higgins, *J. Fluid Mech.* **127**, 103 (1983).
  - [5] R. D. Richtmyer, *Commun. Pure Appl. Math.* **13**, 297 (1960).
  - [6] E. E. Meshkov, *Sov. Fluid Dyn.* **4**, 101 (1969).
  - [7] G. I. Taylor, *Proc. R. Soc. London A* **201**, 192 (1950).
  - [8] U. Alon, J. Hecht, D. Ofer, and D. Shvarts, *Phys. Rev. Lett.* **74**, 534 (1995).
  - [9] H. A. Barnes, *J. Rheol.* **33**, 329 (1989).
  - [10] J. D. Ferry, *Viscoelastic Properties of Polymers* (Wiley, New York, 1961).